Concentration-Dependent Thermodynamics of the Inhibitory Paths in Homogeneous Mn(I) Hydrogenation Catalysis

Yang, Wenjun; Nieuwlands, Erik; Chernyshov, Ivan Yu; Filonenko, Georgy A.; Pidko, Evgeny A.

DOI
10.1002/cctc.202401237

Publication date
2025

Document Version
Final published version

Published in
ChemCatChem

ChemCatChem

Research Article
doi.org/10.1002/cctc.202401237

Chemistry Europe
European Chemical Societies Publishing

www.chemcatchem.org

Concentration-Dependent Thermodynamics of the Inhibitory Paths in Homogeneous Mn(I) Hydrogenation Catalysis

Wenjun Yang,[a, b] Erik Nieuwlands,[b] Ivan Yu. Chernyshov,[b] Georgy A. Filonenko,*[b] and Evgeny A. Pidko*[b]

Dedicated to the memory of Prof. Vladimir B. Kazansky

Many catalytic reactions suffer from product inhibition, which especially hard to control in homogeneous hydrogenation due to the scaling relation between the inhibited and active states of the catalyst. We recently reported one such pathway in Mn(I) hydrogenation and demonstrated that addition of alkoxide bases could affect the thermodynamic favorability of this reaction and selectively suppress the product inhibition. Since external reaction promotors are formally not involved in reaction thermodynamics, we set to investigate the explicit molecular interactions behind these apparently environmental effects. Herein, we reveal that the thermodynamic landscape of the inhibitory process exhibits a non-monotonic dependence on the base concentration. This study related this phenomenon to the presence of two dominant mechanisms operating at different base concentrations. Specifically, the base additives can enhance the ionic strength and lower the free energy of the inhibited state at low promotor concentration. At high base concentrations this study suggested the formation of highly labile alcohol-alkoxide clusters which stabilize the free alcohol and make its addition to the catalyst unfavourable, thereby suppressing the inhibition. While relatively weak, such noncovalent interactions between reactants and reaction environment can cause substantial perturbations to the free energy of catalytic process, ultimately deciding its fate.

The cost of the catalyst represents one of the major hurdles to the practical application of homogeneous catalysis.[1] Improving the performance and lowering catalyst loading required for high conversion is a central topic in catalyst development field. The overall catalytic performance is defined by the interplay of activity and stability of a catalyst with the latter being commonly overlooked.[2] However, the low catalyst stability can decrease its effective concentration during catalytic reaction and limit the catalytic performance, especially at low catalyst loadings.[3] When deactivation is reversible, it manifests as catalyst inhibition which is observed in various homogeneous catalysis settings.[4]

Control over catalyst inhibition is critically important in homogeneous hydrogenation reactions where the lowest possible catalyst loadings are required.[5] High performance hydrogenations are often carried out using bifunctional catalysts that engage in metal-ligand cooperation (MLC) phenomena.[6] Upon the activation with base, these catalysts can generate an acid-base pair that is able to split the hydrogen molecule heterolytically, thus providing hydrogenation-competent species (Figure 1A).

Particularly important in the context of MLC catalysts, the active catalyst form is vulnerable to the attack by acidic compounds (HX), in some cases leading to the inhibition of the catalyst.[7] The intrinsic factor that dictates catalyst speciation and extent of inhibition is the thermodynamic stability of the inhibited state M-X and active state Mn-H. A growing evidence reveals that this inhibition effect is more profound for earth-abundant 3D metal complexes (Fe, Co and Mn) than the noble ones (Ru, Ir, Rh and Os) due to their higher thermodynamic preference to remain in the M-X state.[6d,8] This might result in the inferior performance of 3D-metal-based hydrogenation catalysts. For instance, the extensive thermodynamic studies from Saouma's group found that the M-X was more stable than the M-H for Mn-PNP catalysts, while Ru complexes bearing the same ligand tended to stay in M-H state.[6d,e]

The most common strategy for countering the catalyst inhibition is to elevate the relative free energy of the inhibited state M-X. This is often not trivial due to the presence of linear scaling relation between the free energies of inhibited M-X and active Mn-H for MLC hydrogenation catalysts[7a] which suggests that suppressing the inhibition would simultaneously reduce the catalytic activity. As an alternative, one can tailor the reaction environment to suppress catalyst inhibition— recently, our group identified the metal-alkoxide formation (M-OR) as

[a] Dr. W. Yang
Soochow Institute of Energy and Material Innovations, College of Energy, Soochow University, Suzhou 215006, China

[b] Dr. W. Yang, E. Nieuwlands, I. Y. Chernyshov, Dr. G. A. Filonenko, Prof. Dr. E. A. Pidko
Inorganic Systems Engineering group, Department of Chemical Engineering, Faculty of Applied Sciences, Delft University of Technology, Van der Maasweg 9, Delft 2629 HZ, The Netherlands
E-mail: g.a.filonenko@tudelft.nl
e.a.pidko@tudelft.nl

Supporting information for this article is available on the WWW under https://doi.org/10.1002/cctc.202401237

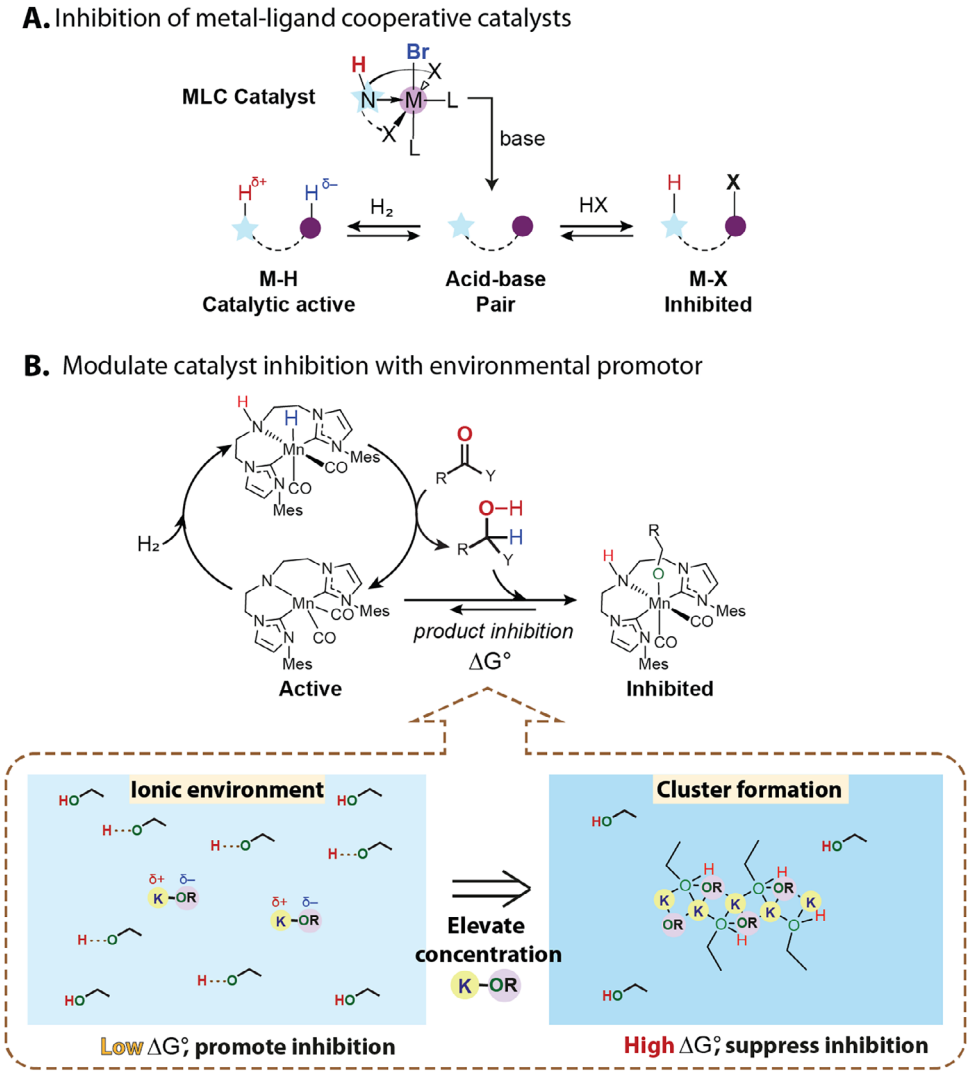

Figure 1. Catalyst inhibition in homogeneous hydrogenation. (A) The competition between hydride formation and inhibition for MLC catalysts; (B) Modulating product inhibition for ester hydrogenation catalyst with basic additives.

the product inhibition pathway in Mn-catalyzed homogeneous ester hydrogenation and utilized basic additives to suppress this inhibition (Figure 1B).[9] We demonstrated that addition of KO^{t}Bu tunes the thermodynamics of the inhibitory equilibrium and makes it unfavourable without altering the activity of the catalyst. In other terms, we found the base to act as an environmental promotor without being directly involved in either bond scission or formation. The explicit nature of molecular interactions between basic promotor and catalytic species however remained unclear. In this work, we conducted a detailed study on the inhibitory equilibrium in the catalytic ensemble of Mn pincer complexes, and identified the presence of two distinct principles enabling opposite environmental perturbations at different concentrations (Figure 1B).

Examining the free energy of the inhibitory equilibrium we found it to show non-monotonic dependence on the concentration of basic additives (Figure 2). We specifically studied the free energy of reversible reaction of alcohol product with the activated amido complex generating metal alkoxide shown in Figure 2, which was proposed to be the product-inhibition pathway in ketone hydrogenation.[9] We selected two representative Mn hydrogenation catalysts based on bis-phosphine amino (PNP) and bis-N-heterocyclic carbene amino (CNC) pincer ligands, and investigated the base concentration dependence of their inhibitory equilibrium ΔG°_{298K} in reaction with ethanol (Figure 2A). The amido complexes **1a** and **2a**, as well as the respective alcohol adducts **1b** and **2b** are coloured and their interconversion can be monitored by temperature-dependent UV-Vis spectroscopy. The reaction free energies ΔG°_{298K} of **1a**-**1b** and **2a**-**2b** transformations were estimated through the temperature dependence of equilibrium composition.

As depicted in Figure 2B, Mn-CNC catalyst **2a** suffers from a more pronounced product inhibition with the measured ΔG°_{298K} being −6.5 kJ/mol, compared to −4.2 kJ/mol for Mn-PNP **1a** in the absence of any base promotor. The free energies were impacted once KO^{t}Bu was added to the mixture. In **1a**-**1b** equilibrium, the increase of base concentration to 0.03 equivalents with respect to ethanol first caused a slight decrease of the Gibbs

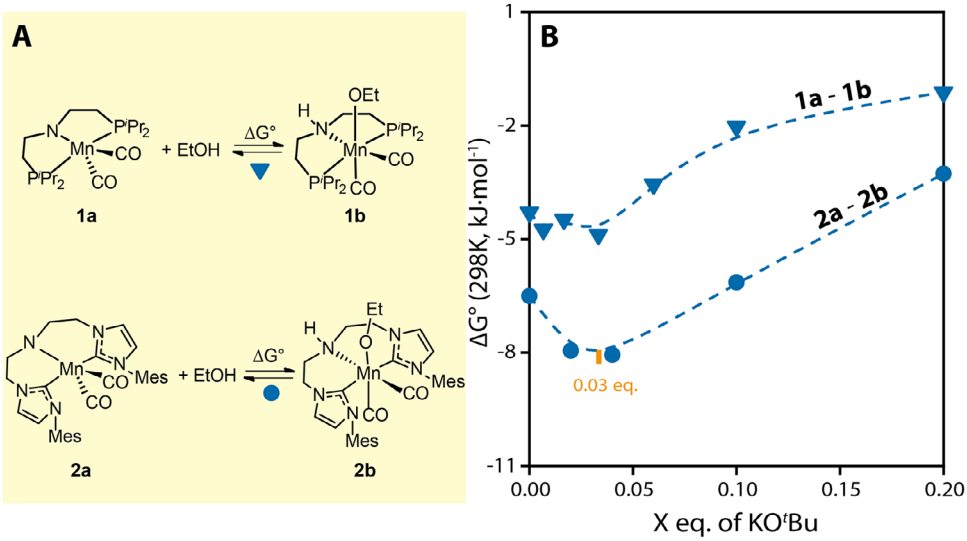

Figure 2. The dependence of the inhibitory equilibria on the concentration of KO^{t}Bu in THF. (A) Inhibitory equilibria **1a**-**1b** and **2a**-**2b**; (B) The plot of Gibbs free energy ΔG°_{298K} versus the X equivanlent of KO^{t}Bu with respect to ethanol. All measurements are performed in THF with 0.837 M EtOH and 1.67 mM metal complex. See Section S3 Supporting Information for conditions.

free energy change down to −4.8 kJ/mol, thereby stabilizing the inhibited alkoxide state of the complex. Free energy then steeply rose up to −1.1 kJ/mol upon further addition of the base (0.03-0.2 eq.). The ΔG°_{298K} of **2a**-**2b** transformation exhibits the same non-monotonic dependence on the base concentration, suggesting the similar interaction mechanism for both catalysts. While adequate amount of the base can effectively suppress product inhibition by elevating its reaction free energy, the current results suggest that the base can also enhance the inhibitory effect of the alcohol at low base concentrations typically used for catalyst activation in homogeneous hydrogenation.

Observing two distinct regimes for free energy variation we assumed that two distinct mechanisms are accessible for the base additives to perturb the reaction free energy. This should be reflected in enthalpy-entropy compensation analysis which is a versatile method for identifying the changes of dominant mechanism in control of systems thermodynamics, widely used for describing biological and chemical processes.[10] Our data plotted as ΔH° versus TΔS° for the **1a**/ethanol system with various amounts of KO^{t}Bu (Figure 3A) confirms the presence of two thermodynamic regimes. Despite the changes of the ΔG°_{298K} were moderate, especially at low base concentrations (Figure 2), the enthalpy varied substantially by ~15 kJ/mol as a function of base concentration. Similar to the ΔG°_{298K} dependence shown in Figure 2, there are two linear enthalpy-entropy compensation regimes with distinct slopes for base loadings in the low concentration range (0-0.03) and at high concentrations (0.06-0.2 eq. to alcohol). The change of the compensation slope suggests a change of dominant mechanism behind free energy perturbation.[10b] Two regimes of enthalpy-entropy compensation are also displayed for **2a**-**2b** pair (Figure 3B), highlighting the generality of observed phenomenon.

Examining the origin of two compensation regimes we examined the literature suggesting that the dilute solutions of alkali alkoxides in their parent alcohol are completely ionized despite the partial covalent character of the alkali-oxygen bond.[11] We therefore assume that the low concentration of base enhances the ionic strength of the environment, which can promote the dissociation of alcohol molecules and the subsequent addition to the amido pincers **1a** and **2a**. This mechanism can indeed be responsible for the initial decrease of the free energy changes for **1a**-**1b** equilibrium at low base loadings.

The nature of free energy increase at high concentrations was further investigated by screening the influence of different additives on the equilibrium in **1a**-**1b** system (Figure 4A). The addition of sodium tetraphenylborate ($NaBPh_4$), which can selectively contribute to ionic strength, resulted in a drop of the ΔG°_{298K} for **1a**-**1b** within the entire examined concentration range. This reveals that the increase of ionic strength does not elevate the free energy of the inhibitory process, but makes it more favorable. Strong bases like potassium bis(trimethylsilyl)amide (KHMDS) significantly elevate the reaction free energy similar to KO^{t}Bu. A minor increase of the free energy was also observed with KOEt. In contrast, strong non-ionic organic base 1,8-diazabicyclo[5.4.0]undec-7-ene (DBU) brings about much smaller changes of the ΔG°_{298K} for **1a**-**1b** compared to other bases. Notably, the strong donor DBU may bind to the Mn complex and hinder the interconversion of **1a**-**1b**, which can also lead to the subtle changes of free energies.

The above screening results find KO^{t}Bu and KHMDS, which are more basic than the conjugate base of EtOH, as the sole additives that are able to elevate the free energy of the inhibitory process. Considering that such strong bases can chemically react with EtOH, one might assume that the deprotonation of the alcohol, resulting in the drop of ethanol concentration, might be the reason behind the free energy increase. However, this is unlikely due to the large excess of alcohol with respect to the base and catalyst employed in this work. We previously demonstrated that such changes in alcohol concentration have negligible effect on ΔG°_{298K}.[9] We therefore assumed that ionic

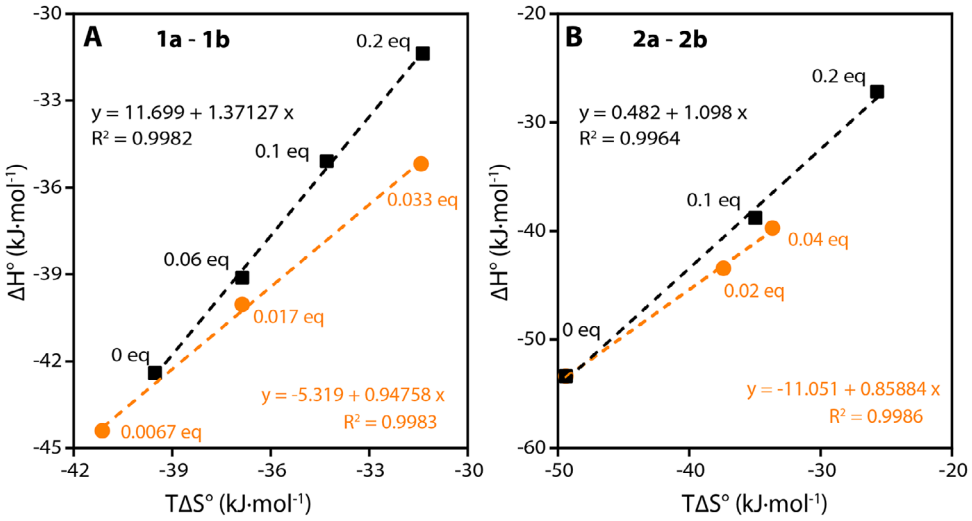

Figure 3. The enthalpy-entropy compensation analysis. (A) ΔH° versus TΔS° plot for equilibriums of **1a**–**1b** with the addition of KO^{t}Bu at T_{hm} (the mean harmonic temperature) = 309.0 K; (B) ΔH° versus TΔS° plot for equilibria of **2a**-**2b** with the addition of KO^{t}Bu at T_{hm} = 314.4 K. The amount of KO^{t}Bu was marked for individual data point as X equivalents.

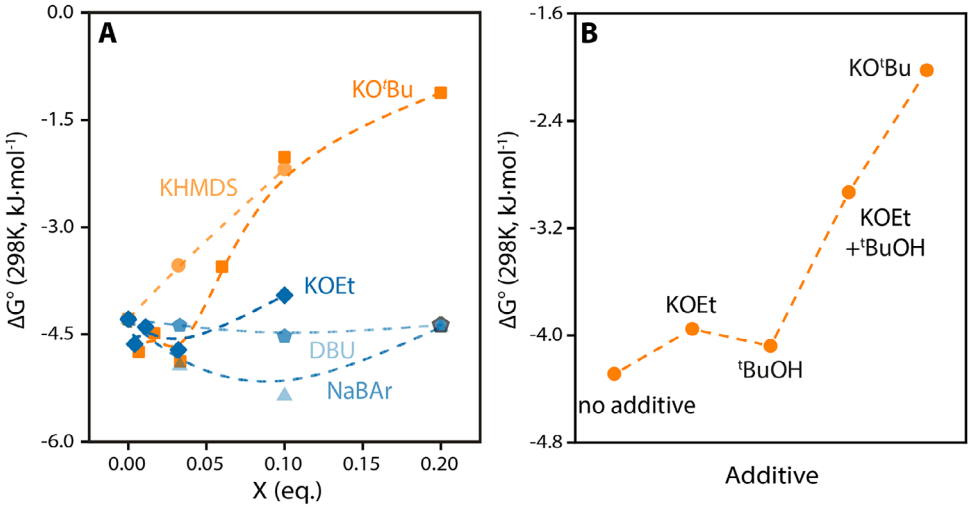

Figure 4. The effects of different additives on the free energy of **1a**-**1b** equilibrium. (A) The plot of ΔG°_{298K} versus the X equivalents of additives with respect to ethanol; (B) The plot of ΔG°_{298K} for different additives (0.1 eq. with respect to ethanol). See S3 of the Supporting Information for conditions.

bases might affect the state of the alcohol in the system. This was hinted by observation that addition of 0.1 equivalents KOEt / ^{t}BuOH mixture increased the ΔG°_{298K} for **1a**-**1b** from −4.2 to −2.9 kJ/mol, very close to the value obtained for pure KO^{t}Bu (Figure 4B). The KOEt or ^{t}BuOH used separately affected the free energy by no more than 0.2 kJ/mol suggesting that both alcohol and alkoxide present at high concentration are needed to affect reaction thermodynamics.

Our data so far suggest that the interaction between the base and the alcohol must contribute to the increase of the inhibition reaction free energy change. Thermodynamic stabilization of alcohol is one of the possible pathways for achieving this. While it is well known that alcohols and alkoxides interact through proton exchange, we sought to explain the base concentration dependence of this reactivity. We speculated that the interaction between alcohol and alkoxide involves the formation of alcohol-alkoxide clusters. The cluster size expands as the base concentration increases, making the alcohol component gradually more stable, thus, prone to disfavour the addition to amido pincer. Such clustering would result in increased size reflected by an increase in the diffusion coefficient (*D*) of ethanol, according to the Stokes-Einstein Gierer-Wirtz Estimation (SEGWE) (Equations 1 and 2).[12]

$$D = \frac{k_B T \left(\frac{3a}{2} + \frac{1}{1+a}\right)}{6\pi\eta\sqrt[3]{\frac{3MW}{4\rho_{eff}N_A}}} \quad (1)$$

$$a = \sqrt[3]{\frac{MW_s}{MW}} \quad (2)$$

where *D* decreases as the solute size increases

Diffusion coefficients of ethanol in the presence of different amounts of base are accessible via DOSY NMR measurements. As shown in Figure S41, the addition of KO^{t}Bu or KHMDS both

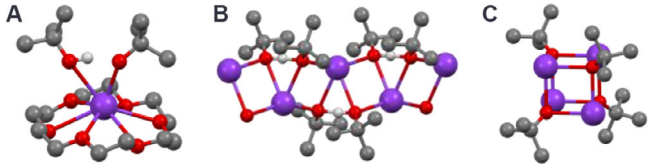

Figure 5. Crystal structures of ^{t}BuOK/^{t}BuOH associates. The balls represent potassium (purple), carbon (gray), oxygen (red), and proton (white) atoms. H—C protons were omitted for clarity. A) Monomeric complex of ^{t}BuOK/^{t}BuOH associate with 18-crown-6 (CSD refcode INUDUS). B) Polymeric form of ^{t}BuOK /^{t}BuOH (SOGKEE). C) Tetramer [^{t}BuOK]$_4$ (SOGKOO).

caused the linear drop of the diffusion coefficient of ethanol from ~2.5·10^{-5}•to ~0.8·10^{-5} cm^2 s. Using the SEGWE equations, the corresponding effective molecular weights can be calculated. The ethanol aggregate in pure THF-d_8 has an MW of 70 amu, which raises significantly to 670 amu in the presence of 0.3 equivanlents of the base. A near 10-fold increase of MW confirmed the substantial expansion of the ethanol aggregate.

Formation of alcohol-alkoxide clusters is well known and references for the explicit molecular models could be found from Cambridge Structure Database.[13] As illustrated in Figure 5, such clusters can be polymeric and have varied ROH/KOR ration in associates. For example coprecipitation of dilute ^{t}BuOK/^{t}BuOH solution with 18-crown-6 gives an isolated ionic pair K[^{t}BuOH···O^{t}Bu] (Figure 5A).[14] Co-crystallization of equal amounts of KO^{t}Bu and ^{t}BuOH generates polymeric [^{t}BuOK···HO^{t}Bu]$_n$ chains, containing the bond ^{t}BuOH·in the repeating unit (Figure 5B).[15] One can speculate that K[ROH···OR] pairs and [ROK···HOR]$_n$ chains are the two associate forms forming as the concentration of ROK increases to a level comparable to that of ROH. Finally, the precipitation of pure ^{t}BuOK gives a cubic cluster with K and O atoms forming interpenetrating tetrahedra [^{t}BuOK]$_4$, which is anticipated to be the dominant associate at low alcohol concentrations (Figure 5C).[16] In case of our system, where the [KOR] < [ROH], we envision the formation of oligomeric chain-like KOR/ROH clusters, which grow as [KOR] elevates. This is in agreement with the above diffusion data that show the expansion of the cluster size. It is worth noting that the suggested ROH/KOR associates are highly labile and can have different structures in solution.

We further simulated the thermodynamics for the oligomerization of monomeric to oligomeric KOR/ROH via density functional theory (DFT) computations (for details see Section S6 of the Supporting Information). The free energy changes for the generation of dimer, trimer and tetramer are −17, −20 and −22 kJ/mol respectively, confirming the oligomerization as a thermodynamically favorable process. The clustering results of KOR/ROH suggest that dynamic composition of catalytic reaction mixture gradually changes and is, indeed, condition dependent. The elevated free energies of inhibitory amido complex–alcohol adduct equilibrium, therefore, should stem from the gradual stabilization of free alcohol in the alcohol-alkoxide clusters which affect thermodynamics of the inhibitory reaction once base concentrations become sufficiently high.

In summary, we describe the details of the equilibrium free energy perturbations which steer the inhibition of 3d-TM MLC hydrogenation catalysts. We demonstrate that the gradual agglomeration of alcohol product into alcohol-alkoxide oligomers is the main mechanism behind free energy tuning which ultimately protects the catalyst from inhibition. Since the alcohol clustering can only be affected at high base promotor loadings, we conclude that it is a strict requirement for preventing the product inhibition in Mn catalysts prone to formation of stable metal alkoxide complexes. These trends are a part of more complex inhibition pattern where alcohol clustering is preceded by ionic effects detrimental for catalysis that base promotors show at small concentration. Since our experiments make use of common Mn pincer catalysts under typical reaction conditions, we point out that analysis of reaction mixture dynamics has a nearly unexplored potential for studying and improving the performance of these catalysts and would hopefully become a standard practice in this field.

Acknowledgements

This research was supported by the European Research Council under the European Union's Horizon 2020 research and innovation program (grant agreement No. 725686). The authors also thank NWO Domain Science for the use of the national supercomputer facilities. IYC thanks Dr. Evgeny Uslamin for the computational discussions.

Conflict of Interests

The authors declare no conflict of interest.

Data Availability Statement

The data that support the findings of this study are available in the supplementary material of this article.

Keywords: Basic promotor · Catalyst deactivation · Enthalpy-entropy compensation · Free energy perturbations · Homogeneous Hydrogenation

[1] a) H. Shimizu, N. Sayo, T. Saito, in *Asymmetric Catalysis on Industrial Scale: Challenges, Approaches and Solutions*, Wiley & Sons, Inc, Hoboken, NJ, **2010**, pp. 207–218; b) I. T. Horváth, E. Iglesia, M. T. Klein, J. A. Lercher, A. J. Russell, E. I. Stiefel, *Encyclopedia of catalysis*, *6*, John Wiley & Sons, Inc, Hoboken, N J **2003**; c) J. G. d. Vries, A. H. M. d. Vries, *Eur. J. Org. Chem.* **2003**, *2003*, 799–811.
[2] W. Yang, G. A. Filonenko, E. A. Pidko, *Chem. Commun.* **2023**, *59*, 1757–1768.
[3] R. H. Crabtree, *Chem. Rev.* **2015**, *115*, 127–150.
[4] a) D. Heller, A. H. M. De Vries, J. G. De Vries, in *The Handbook of Homogeneous Hydrogenation*, Wiley-VCH, Weinheim, **2006**, pp. 1483–1516; b) A. Barbieri, J. B. Kasper, F. Mecozzi, O. Lanzalunga, W. R. Browne, *ChemSusChem* **2019**, *12*, 3126–3133; c) D. E. Chapple, P. D. Boyle, J. M. Blacquiere, *ChemCatChem* **2021**, *13*, 3789–3800.
[5] a) J. Magano, J. R. Dunetz, *Org. Proc. Res. Dev.* **2012**, *16*, 1156–1184; b) F. J. McQuillin, *Homogeneous hydrogenation in organic chemistry*, Vol. *1*, Springer Science & Business Media, Berlin **2012**; c) P. A. Chaloner, M. A. Esteruelas, F. Joó, L. A. Oro, *Homogeneous hydrogenation*, Vol. *15*,

Springer Science & Business Media, Berlin **2013**; d) C. S. Seo, R. H. Morris, *Organometallics* **2018**, *38*, 47–65.
[6] a) J. R. Khusnutdinova, D. Milstein, *Angew. Chem., Int. Ed.* **2015**, *54*, 12236–12273; b) G. A. Filonenko, R. van Putten, E. J. Hensen, E. A. Pidko, *Chem. Soc. Rev.* **2018**, *47*, 1459–1483; c) K. Das, S. Waiba, A. Jana, B. Maji, *Chem. Soc. Rev.* **2022**, *51*, 4386–4464; d) C. L. Mathis, J. Geary, Y. Ardon, M. S. Reese, M. A. Philliber, R. T. VanderLinden, C. T. Saouma, *J. Am. Chem. Soc.* **2019**, *141*, 14317–14328; e) K. Schlenker, E. G. Christensen, A. A. Zhanserkeev, G. R. McDonald, E. L. Yang, K. T. Lutz, R. P. Steele, R. T. VanderLinden, C. T. Saouma, *ACS. Catal.* **2021**, *11*, 8358–8369.
[7] a) L. Artús Suàrez, D. Balcells, A. Nova, *Top. Catal.* **2022**, *65*, 82–95; b) D. H. Nguyen, X. Trivelli, F. d. r. Capet, J.-F. o. Paul, F. Dumeignil, R. g. M. Gauvin, *ACS. Catal.* **2017**, *7*, 2022–2032; c) A. Passera, A. Mezzetti, *Adv. Synth. Catal.* **2019**, *361*, 4691–4706; d) C. S. Seo, B. T. Tsui, M. V. Gradiski, S. A. Smith, R. H. Morris, *Catal. Sci. Technol.* **2021**, *11*, 3153–3163; e) A. M. Krieger, V. Sinha, A. V. Kalikadien, E. A. Pidko, *Z. Anorg. Allg. Chem.* **2021**, *647*, 1486–1494.
[8] a) K. Abdur-Rashid, S. E. Clapham, A. Hadzovic, J. N. Harvey, A. J. Lough, R. H. Morris, *J. Am. Chem. Soc.* **2002**, *124*, 15104–15118; b) R. J. Hamilton, S. H. Bergens, *J. Am. Chem. Soc.* **2006**, *128*, 13700–13701.
[9] W. Yang, T. Y. Kalavalapalli, A. M. Krieger, T. A. Khvorost, I. Y. Chernyshov, M. Weber, E. A. Uslamin, E. A. Pidko, G. A. Filonenko, *J. Am. Chem. Soc.* **2022**, *144*, 8129–8137.
[10] a) L. Liu, Q.-X. Guo, *Chem. Rev.* **2001**, *101*, 673–696; b) F. Martínez, M. Á. Peña, P. Bustamante, *Fluid Phase Equilib.* **2011**, *308*, 98–106; c) D. R. Delgado, E. M. Mogollon-Waltero, C. P. Ortiz, M. Á. Peña, O. A. Almanza, F. Martínez, A. Jouyban, *J. Mol. Liq.* **2018**, *271*, 522–529.
[11] M. S. Bains, *Can. J. Chem.* **1964**, *42*, 945–946.
[12] B. Tang, K. Chong, W. Massefski, R. Evans, *J. Phys. Chem. B* **2022**, *126*, 5887–5895.
[13] C. R. Groom, I. J. Bruno, M. P. Lightfoot, S. C. Ward, *Acta. Cryst. B.* **2016**, *72*, 171–179.
[14] P. Jacqueline, K. Christian, 1484254: Experimental Crystal Structure Determination, **2016**, https://doi.org/10.5517/ccdc.csd.cc1lth52.
[15] M. H. Chisholm, S. R. Drake, A. A. Naiini, W. E. Streib, *Polyhedron* **1991**, *10*, 337–345.
[16] P. A. Dub, N. V. Tkachenko, *J. Phys. Chem. A.* **2021**, *125*, 5726–5737.

Manuscript received: July 19, 2024
Revised manuscript received: September 13, 2024
Accepted manuscript online: September 13, 2024
Version of record online: September 26, 2024